IJIRSET
International Journal of Innovative Research in
SCIENCE | ENGINEERING | TECHNOLOGY

e-ISSN: 2319-8753 | p-ISSN: 2347-6710

INTERNATIONAL JOURNAL OF INNOVATIVE RESEARCH

IN SCIENCE | ENGINEERING | TECHNOLOGY

Volume 13, Issue 9, September 2024

INTERNATIONAL STANDARD SERIAL NUMBER INDIA

Impact Factor: 8.524

9940 572 462 | 6381 907 438 | ijirset@gmail.com | www.ijirset.com

International Journal of Innovative Research of Science, Engineering and Technology (IJIRSET)

Impact Factor 8.524

|www.ijirset.com |A Monthly, Peer Reviewed & Referred Journal| e-ISSN: 2319-8753| p-ISSN: 2347-6710|

Volume 13, Issue 9, September 2024

|DOI: 10.15680/IJIRSET.2024.1309044|

Structural and Phase Study of $Co_{1-x}Zn_xFe_2O_4$ (x = 0.4) Nanoparticles with Magnetic Analysis

Ram S. Barkule[1], Mahendra D. Shelar[2], Sudarshana G. Badhe[3]

Department of Physics, Sundarrao More Arts, Commerce and Science College, Poladpur, Raigad, India[1]

Department of Chemistry, Rajarshi Shahu Art's, Commerce and Science College, Pathri, India[2]

Department of Physics, R.B. Attal Arts, Science and Commerce College, Georai, Beed, India[3]

ABSTRACT: This research details the synthesis and characterization of $Co_{0.6}Zn_{0.4}Fe_2O_4$ nanoparticles achieved through a wet chemical approach. The resulting nanoparticles were analyzed using X-ray diffraction (XRD), Fourier-transform infrared spectroscopy (FTIR), and direct current (DC) resistivity measurements. The XRD results confirmed the establishment of a single-phase cubic spinel structure. FTIR analysis revealed absorption peaks associated with metal-oxygen bond vibrations. The DC resistivity measurements suggested a thermally activated conduction mechanism. Furthermore, magnetic analysis indicated ferromagnetic characteristics, exhibiting notable saturation magnetization, coercivity, and remanent magnetization. These findings underscore the potential applications of $Co_{0.6}Zn_{0.4}Fe_2O_4$ nanoparticles in diverse areas such as semiconductor technology, nanosensors, and biomedical devices.

KEYWORDS: X-ray diffraction; SEM; DC-electric resistivity; Magnetic Property.

I. INTRODUCTION

Spinel ferrites have the general formula MFe_2O_4, where M represents a divalent metal cation such as Fe^{2+}, Co^{2+}, Ni^{2+}, Cu^{2+}, Mg^{2+}, or Zn^{2+}. The formula can be expanded to $(Me_{2+1-x}Fe_{3+x})[Me_{2+x}Fe_{3+2-x}]O_4$, where the cation distribution within the crystal lattice defines the type of cubic structure: normal, inverse, or mixed spinel [1]. The crystal structure of spinel ferrites is characterized by a unit cell that is derived from a cubic close-packed configuration of oxygen anions. This arrangement provides 64 tetrahedral (A) sites and 32 octahedral (B) sites available for cation occupancy. However, due to the chemical stoichiometry of the material, only a portion of these sites are actually filled. Typically, within a single unit cell, 8 out of the 64 A sites and 16 out of the 32 B sites are occupied by metal cations [2]. The oxygen position parameter, commonly represented as u, is vital in influencing the structural and physical characteristics of spinel ferrites. These materials, characterized by the general formula MFe_2O_4, crystallize in a cubic lattice where oxygen anions (O^{2-}) are arranged in a close-packed configuration. The specific arrangement of these anions has a significant impact on the geometry of the cation sublattice, thereby affecting various material properties, including magnetic ordering, electrical conductivity, and catalytic activity. In an ideal spinel structure, the oxygen anions are symmetrically arranged within the unit cell; however, actual crystals frequently display minor deviations from this ideal configuration [3]. The oxygen parameter (u) quantifies the displacement of oxygen atoms from their ideal positions along the body diagonal of the unit cell. This parameter directly affects the distances between cations and oxygen anions, consequently influencing the bond lengths and angles between the metal cations located at both tetrahedral (A) and octahedral (B) sites [4]. These minor alterations in the position of oxygen can alter the strength of superexchange interactions among cations, particularly those at the B sites, which are essential for determining magnetic properties. Changes in the oxygen position parameter can also affect the lattice constant and the electronic structure of spinel ferrites, thereby modifying their dielectric and optical properties. A comprehensive understanding of the oxygen position parameter is crucial for optimizing the material's properties for targeted applications [5]. This parameter can be manipulated through various synthesis methods, doping with alternative cations, or thermal treatments. Even slight variations in the (u) parameter, particularly within the range of 0.25 to 0.27, can lead to substantial changes in the overall performance of the spinel ferrite, underscoring its importance. In a normal spinel structure, divalent cations, such as Fe^{2+}, Zn^{2+}, or Co^{2+}, tend to occupy the tetrahedral (A) sites, where they are coordinated by four oxygen anions in a tetrahedral geometry [6]. Conversely, the octahedral [B] sites, which are surrounded by six oxygen anions, are filled by trivalent cations, such as Fe^{3+}. This specific cation distribution plays a significant role in determining the magnetic and electronic characteristics of the material. In an inverse spinel structure, the distribution of cations is altered; trivalent cations (e.g., Fe^{3+}) occupy the tetrahedral (A) sites, while both divalent and trivalent cations occupy

International Journal of Innovative Research of Science, Engineering and Technology (IJIRSET)

Impact Factor 8.524

|www.ijirset.com |A Monthly, Peer Reviewed & Referred Journal| e-ISSN: 2319-8753| p-ISSN: 2347-6710|

Volume 13, Issue 9, September 2024

|DOI: 10.15680/IJIRSET.2024.1309044|

the octahedral [B] sites. This combination of different valence states in the [B] sites can lead to distinctive magnetic interactions, as the exchange coupling among the various cations affects the magnetic ordering of the material [7, 8]. The differing cation distributions between (A) and [B] sites in normal and inverse spinels result in unique structural and magnetic properties, which are essential for their use in applications such as catalysis, electronics, and magnetic storage devices. Additionally, external factors like temperature, synthesis techniques, and doping can influence the arrangement of cations, resulting in variations in the physical properties of spinel ferrites [9]. Cobalt ferrite ($CoFe_2O_4$) exhibits an inverse spinel structure, with trivalent iron ions (Fe^{3+}) in the A sites and both divalent cobalt ions (Co^{2+}) and trivalent iron ions (Fe^{3+}) in the [B] sites. The oxygen anions form a face-centered cubic lattice. Zinc ferrite ($ZnFe_2O_4$) is another important spinel ferrite. Nanosized $ZnFe_2O_4$ powders synthesized via the sol-gel auto-combustion method showed that as the annealing temperature increases, Fe^{3+} cations filling the B sites are gradually reduced to Fe^{2+} cations, likely due to the oxidation of Zn^{2+} to Zn^{3+}. Substitution of divalent cations in spinel ferrites can significantly alter their properties. For example, in Zn-doped $CoFe_2O_4$ nanoparticles, the lattice parameter increases gradually as the Zn concentration increases from x = 0.0 to x = 0.8. The spontaneous magnetization also increases monotonically from ~51 emu/g for x = 0.0 to ~106 emu/g for x = 0.8. Spinel ferrites exhibit a wide range of useful properties, including thermal and chemical stability, unique structural and magnetic characteristics, and potential applications in photocatalysis, biosensors, catalysis, magnetic refrigeration, permanent magnets, drug delivery, and hyperthermia treatment [10-13]. These scientific data highlight the versatility and tunability of spinel ferrites, making them attractive materials for various technological applications. The ability to control their composition, structure, and properties through doping and synthesis methods enables the development of optimized materials for specific uses.

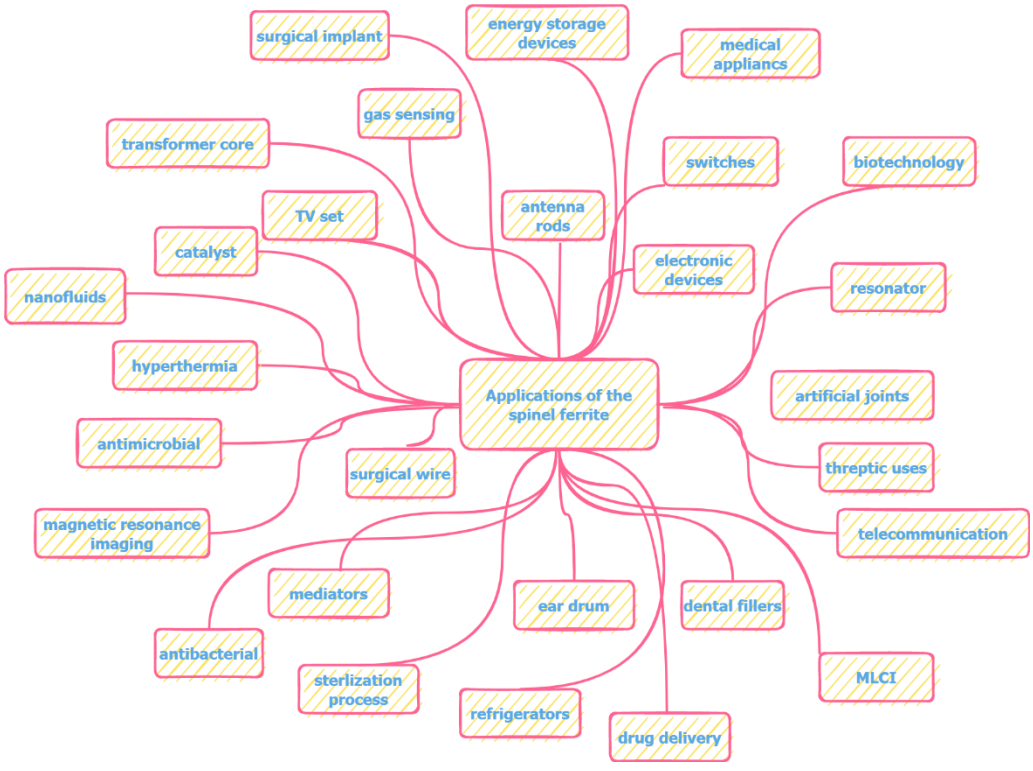

Figure 1 Various Applications of Spinel Ferrite

II. EXPERIMENTAL METHOD

Materials:

The For the synthesis of spinel-structured $Co_{1-x}Zn_xFe_2O_4$ nanoparticles with varying compositions where x = 0.3, high-purity starting materials were utilized without further purification. These materials included cobalt nitrate hexahydrate ($Co(NO_3)_2 \cdot 6H_2O$), zinc nitrate tetrahydrate ($Zn(NO_3)_2 \cdot 4H_2O$), and ferric nitrate nonahydrate ($Fe(NO_3)_3 \cdot 9H_2O$), each with a purity of 99.9%. The synthesis process involved the use of citric acid as a complexing agent to facilitate the

International Journal of Innovative Research of Science, Engineering and Technology (IJIRSET)

Impact Factor 8.524

|www.ijirset.com |A Monthly, Peer Reviewed & Referred Journal| e-ISSN: 2319-8753| p-ISSN: 2347-6710|

Volume 13, Issue 9, September 2024

|DOI: 10.15680/IJIRSET.2024.1309044|

formation of the desired spinel structure. The ratio of metal nitrates to the fuel ($C_6H_5O_7^{3-}$) was carefully maintained at 1:3 to ensure optimal reaction conditions. This specific ratio helps to create a stable metal-citrate complex, which is crucial for the formation of homogeneous and well-defined nanoparticles. Furthermore, ammonia solution (NH_4OH) was employed to adjust and stabilize the pH at 8 throughout the synthesis. Maintaining a controlled pH is crucial for achieving the desired properties and composition of the nanoparticles, as it influences the solubility and stability of the metal-citrate complexes. This precise approach allows for fine-tuning of the nanoparticles' composition and properties, contributing to the successful production of $Co_{1-x}Zn_xFe_2O_4$ nanoparticles with tailored characteristics for various applications. By utilizing high-purity starting materials, optimizing the metal nitrate to citric acid ratio, and carefully controlling the pH during synthesis, researchers can effectively produce spinel-structured $Co_{1-x}Zn_xFe_2O_4$ nanoparticles with desired compositions and properties. This level of control is essential for developing advanced materials with specific applications in mind, such as in the fields of catalysis, energy storage, and magnetic devices.

III. SYNTHESIS OF $CO_{1-X}ZN_XFE_2O_4$ (X=0.4) NANOPARTICLES

Synthetic route:

The The wet chemical synthesis method was developed to produce $Co_{1-x}Zn_xFe_2O_4$ (x=0.4) nanoparticles (NPs), which are of significant interest due to their unique magnetic and electrical properties, making them suitable for various applications in fields such as catalysis, energy storage, and biomedical technologies. The synthesis began with the careful selection of high-purity starting materials. Metal nitrates of cobalt ($Co(NO_3)_2{\cdot}6H_2O$) and ferric ($Fe(NO_3)_3{\cdot}9H_2O$), both with a purity of 99.9%, were combined in a beaker with an adequate amount of deionized (DI) water. The choice of deionized water is crucial, as it eliminates impurities that could interfere with the synthesis process and the final properties of the nanoparticles. Once the metal nitrates were added to the DI water, the resulting solution was thoroughly stirred and homogenized using a magnetic hot-plate stirrer. This step ensures that the metal ions are evenly distributed throughout the solution, which is essential for achieving a uniform composition in the final product. To facilitate the formation of the desired spinel structure, a 1:3 ratio of metal nitrates to citric acid ($C_6H_5O_7^{3-}$) was employed as the complexing agent. Citric acid plays a vital role in stabilizing the metal ions in solution and promoting the formation of metal-citrate complexes, which are critical for the subsequent steps in the synthesis. To drive off excess water and concentrate the solution, the hot-plate temperature was set to 80°C for a duration of 3 hours. This controlled heating process allows for the gradual evaporation of water, leading to an increase in the concentration of the metal-citrate complexes in the solution. During the synthesis, ammonia solution (NH_4OH) was gradually added to maintain the solution's pH at 8. Controlling the pH is essential for ensuring the stability of the metal-citrate complexes and promoting the formation of the desired gel structure. A pH of around 8 is optimal for the precipitation of metal hydroxides, which will later contribute to the formation of the nanoparticles. As the process continued, the solution transitioned from a ‘sol’ (a colloidal suspension) to a ‘gel’ state, eventually forming a ‘viscous brown gel.’ This transformation indicates the successful formation of a network of metal hydroxides and citric acid, which will serve as the precursor for the nanoparticles. In the final stage of the synthesis, increased ionic exchange within the system led to the release of gaseous byproducts, such as water vapor and carbon dioxide. This release of gases is a critical indicator of the progress of the reaction. To facilitate the self-propagating auto-combustion process, the temperature was raised to 110°C. This increase in temperature initiates a rapid exothermic reaction that leads to the combustion of the organic components, resulting in the formation of a loose powder of pre-sintered $Co_{1-x}Zn_xFe_2O_4$ (x=0.4). The auto-combustion process is advantageous as it produces nanoparticles with a high degree of homogeneity and fine control over their size and morphology. The resulting sintered $Co_{1-x}Zn_xFe_2O_4$ (x=0.4) nanoparticles possess unique properties that can be tailored by adjusting the synthesis parameters, such as the concentration of metal nitrates, the ratio of citric acid, and the pH of the solution. The wet chemical synthesis method, particularly the sol-gel auto-combustion approach, offers several advantages, including simplicity, cost-effectiveness, and the ability to produce nanoparticles with narrow size distributions. These characteristics make sintered $Co_{1-x}Zn_xFe_2O_4$ (x=0.4) nanoparticles highly suitable for various applications, including magnetic materials, catalysis, and advanced electronic devices. Ongoing research aims to further explore and optimize the synthesis process to enhance the performance and applicability of these nanoparticles in emerging technologies.

International Journal of Innovative Research of Science, Engineering and Technology (IJIRSET)

Impact Factor 8.524

|www.ijirset.com |A Monthly, Peer Reviewed & Referred Journal| e-ISSN: 2319-8753| p-ISSN: 2347-6710|

Volume 13, Issue 9, September 2024

|DOI: 10.15680/IJIRSET.2024.1309044|

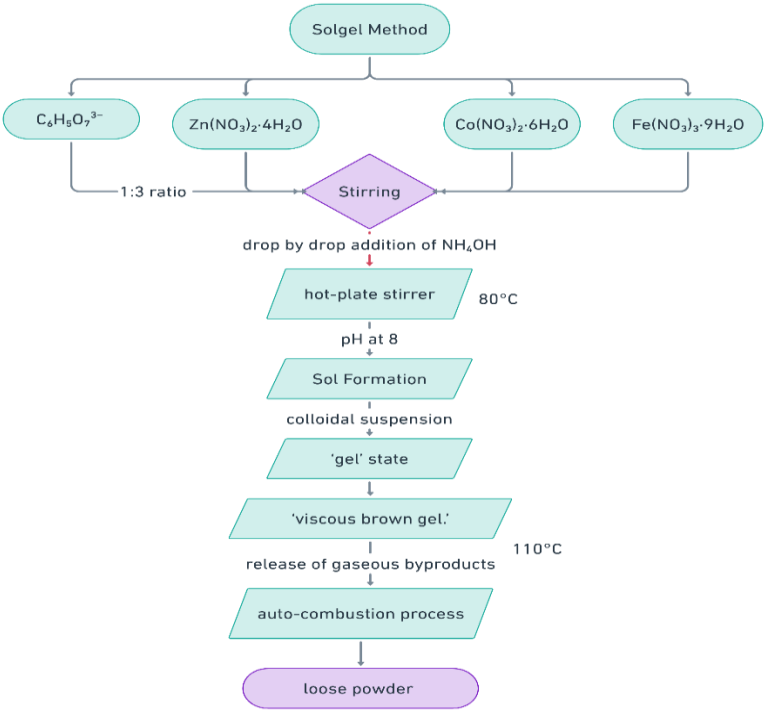

Figure 2 General Synthetic route for $Co_{1-x}Zn_xFe_2O_4$ (x=0.4) nanoparticles via solgel auto-combustion method

IV. RESULTS AND DISCUSSION

X-ray diffraction

The Structural investigations of $CoZnFe_2O_4$ nanoparticles (NPs) were conducted using X-ray diffraction (XRD) with a X'PertPRO MPD PANalytical system. The analysis spanned a 2θ range from 20º to 80º, utilizing Cu-Kα radiation with a wavelength of λ = 1.5405 Å at room temperature. The XRD pattern, illustrated in Figure 1, indicates that the $CoZnFe_2O_4$ NPs exhibit a single-phase cubic spinel structure [14], with no secondary peaks detected (see Figure 2). The diffraction pattern confirmed the presence of specific planes, including (220), (311), (400), (422), (511), (440), and (622), [15] as detailed in **Table 1**.

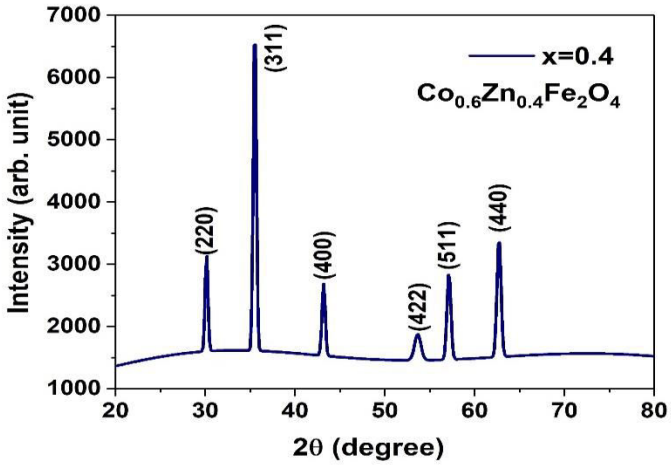

Figure 3. X-ray diffraction pattern of $Co_{1-x}Zn_xFe_2O_4$ (x=0.4) nanoparticles

International Journal of Innovative Research of Science, Engineering and Technology (IJIRSET)

Impact Factor 8.524

|www.ijirset.com |A Monthly, Peer Reviewed & Referred Journal| e-ISSN: 2319-8753| p-ISSN: 2347-6710|

Volume 13, Issue 9, September 2024

|DOI: 10.15680/IJIRSET.2024.1309044|

Table 1. Miller indices of the $Co_{1-x}Zn_xFe_2O_4$ nanoparticles sample x = 0.4

h	k	l	2θ	θ	Sinθ	2Sinθ	d	(a/d)^2	a
2	2	0	30.135	15.067	0.260	0.520	2.962	8.002	8.379
3	1	1	35.512	17.756	0.305	0.610	2.525	11.012	8.375
4	0	0	43.172	21.586	0.368	0.736	2.093	16.026	8.373
4	2	2	53.658	26.829	0.451	0.903	1.706	24.120	8.359
5	1	1	57.132	28.566	0.478	0.956	1.611	27.074	8.369
4	4	0	62.709	31.355	0.520	1.041	1.480	32.059	8.372
6	2	2	73.590	36.795	0.599	1.198	1.286	42.478	8.529
									8.394

The data from **Table 1** provide critical insights into the structural characteristics of $Co_{0.6}Zn_{0.4}Fe_2O_4$ nanoparticles, particularly in terms of their crystallographic planes, lattice spacing, and overall crystal structure. The Miller indices (h, k, l) along with the diffraction angles (2θ and θ) show that the interplanar spacing (d) decreases as the diffraction angle increases, which is typical for a cubic spinel structure. The calculated lattice constant (a) remains nearly uniform across different planes, averaging around 8.394 Å, suggesting that the sample retains a stable cubic lattice. This consistency in lattice constant confirms the structural integrity of the $Co_{0.6}Zn_{0.4}Fe_2O_4$ nanoparticles.

Table 2. FWHM, Crystallite size (D), dislocation density (δ), lattice strain (ε), of $Co_{1-x}Zn_xFe_2O_4$ nanoparticles sample x = 0.4

2θ	θ in Degree	Radian(θ)	FWHM Degree (θ)	FWHM Radian (θ)	Cos θ	D= 0.9λ/βCosθ	D nm	$\delta*10^3$ (nm^{-2})	$\varepsilon*10^{-3}$
30.135	15.06727	0.263	0.37049	0.006	0.966	222.194	22.219	2.025	0.435
35.512	17.75597	0.310	0.39693	0.007	0.952	210.278	21.028	2.261	0.554
43.172	21.58581	0.377	0.42363	0.007	0.930	201.786	20.179	2.455	0.731
53.658	26.82887	0.468	0.82033	0.014	0.892	108.580	10.858	8.481	1.810
57.132	28.565975	0.498	0.50409	0.009	0.878	179.530	17.953	3.102	1.197
62.709	31.35453	0.547	0.52306	0.009	0.854	177.937	17.794	3.158	1.390
73.590	36.795205	0.642	0.49488	0.009	0.801	200.545	20.055	2.486	1.615
							18.584		

In **Table 2**, the crystallite size (D) and other related parameters, such as dislocation density (δ) and lattice strain (ε), offer valuable information on the crystal quality and defects. The crystallite size decreases at higher diffraction angles, indicating the presence of smaller crystallites or more pronounced peak broadening at these reflections. The dislocation density increases correspondingly, suggesting a higher concentration of defects in smaller crystallites. Furthermore, lattice strain values rise with increasing 2θ, indicating that the material experiences more distortion at higher angles. These factors, including the moderate levels of dislocation and strain, help to understand the material's structural imperfections, which can significantly influence its magnetic and electronic properties. Overall, this analysis highlights the interconnectedness of structural parameters and their role in determining the functional behavior of spinel ferrites.

Infra-red Spectroscopy

The FTIR spectra for $Co_{1-x}Zn_xFe_2O_4$ (x=0.4) nanoparticles with a composition of (x = 0.4), as presented in **Figure 4**, show several key absorption peaks that offer valuable information regarding the structural and chemical characteristics of the material. The presence of these peaks confirms the formation of spinel ferrite structures and provides details on the interactions between the metal cations and oxygen in the crystal lattice [16]. The first absorption band (ν_1) appears at approximately 545 cm^{-1}, which is characteristic of the stretching vibrations of metal-oxygen (M-O) bonds at the tetrahedral sites. In spinel ferrites, this band is often associated with the higher-energy vibrations that occur when

International Journal of Innovative Research of Science, Engineering and Technology (IJIRSET)

Impact Factor 8.524

|www.ijirset.com |A Monthly, Peer Reviewed & Referred Journal| e-ISSN: 2319-8753| p-ISSN: 2347-6710|

Volume 13, Issue 9, September 2024

|DOI: 10.15680/IJIRSET.2024.1309044|

cations such as Co^{2+} or Fe^{3+} are positioned at tetrahedral coordination sites. The position and intensity of this peak provide insights into the cation distribution at these sites, suggesting a stable tetrahedral coordination despite the partial substitution of Zn^{2+} in the structure. The second absorption band (ν_2) is observed at a lower wavenumber, around 403 cm^{-1}, which corresponds to the metal-oxygen stretching vibrations at the octahedral sites [17]. In this case, the cations located in octahedral coordination, such as Zn^{2+}, Fe^{3+}, or Co^{2+}, contribute to this band. The lower frequency of these vibrations is due to the larger size and weaker bonds at the octahedral sites compared to those at the tetrahedral positions. The shift in the absorption bands, especially with the introduction of Zn^{2+}, indicates that Zn is successfully incorporated into the lattice, altering the local bonding environment and affecting the vibrational frequencies. This is further supported by the changes in intensity and position of the bands, which reflect the substitution-induced distortions in the crystal structure [18]. The differences in cation size and bonding strength between Zn^{2+} and Co^{2+}/Fe^{3+} modify the M-O bond lengths and angles, leading to observable changes in the FTIR spectra. These findings from the FTIR spectra are significant, as they confirm the structural integrity of the spinel ferrite and provide insights into the material's chemical composition and bonding. The successful incorporation of Zn into the $CoFe_2O_4$ lattice has implications for tuning the physical and magnetic properties of the nanoparticles, making them suitable for a wide range of applications such as in catalysis, magnetic data storage, and biomedical fields. By understanding the vibrational properties and the effects of Zn substitution, researchers can optimize the synthesis process and improve the performance of these ferrite nanoparticles in various technological applications.

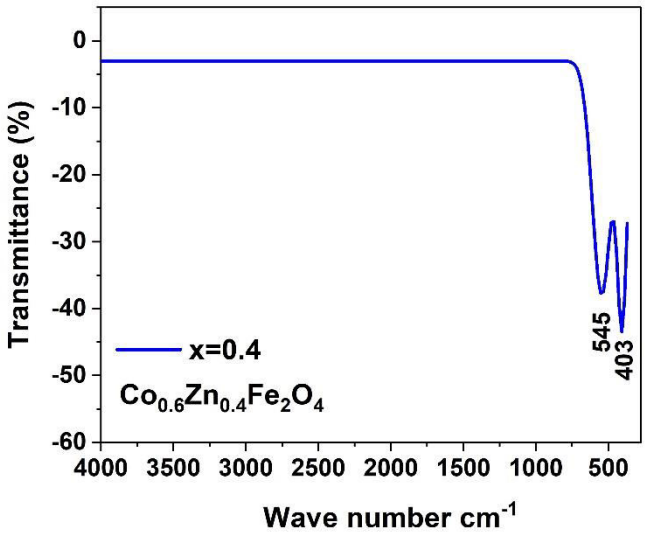

Figure 4 FTIR spectra of $Co_{1-x}Zn_xFe_2O_4$ (x=0.4) nanoparticles

DC resistivity

The DC resistivity graph for $Co_{1-x}Zn_xFe_2O_4$ nanoparticles with a composition of (x = 0.4) provides valuable information about the material's electrical properties. Figure 5 shows the natural logarithm of electrical conductivity (log σ) plotted against the reciprocal of temperature (1000/T in Kelvin), demonstrating a clear temperature dependence. As temperature increases (moving from right to left along the x-axis), electrical conductivity rises, indicating a decrease in resistivity. This relationship follows an Arrhenius-type behavior, where conductivity increases exponentially with temperature. The slope of this line can be used to calculate the activation energy (Ea) for conduction, based on the Arrhenius equation [19]:

$$\sigma = \sigma_0 \exp(\frac{E_a}{kT}) \quad (1)$$

This behavior suggests that conduction in the material is thermally activated, characteristic of semiconductors, where charge carriers gain sufficient thermal energy to overcome the activation energy barrier. The specific composition of $Co_{0.6}Zn_{0.4}Fe_2O_4$ indicates that Zn substitution plays a significant role in the conduction mechanism. Zn ions, which have a different electronic configuration compared to Co ions, alter the electronic structure and impact the activation

International Journal of Innovative Research of Science, Engineering and Technology (IJIRSET)

Impact Factor 8.524

|www.ijirset.com |A Monthly, Peer Reviewed & Referred Journal| e-ISSN: 2319-8753| p-ISSN: 2347-6710|

Volume 13, Issue 9, September 2024

|DOI: 10.15680/IJIRSET.2024.1309044|

energy for conduction. This substitution affects factors such as the density of states, charge carrier mobility, and the crystal structure, thereby influencing the overall conductivity. The DC resistivity graph confirms that $Co_{0.6}Zn_{0.4}Fe_2O_4$ exhibits thermally activated semiconducting behavior, with conductivity increasing with temperature, highlighting the effect of Zn substitution on the material's electrical properties [20].

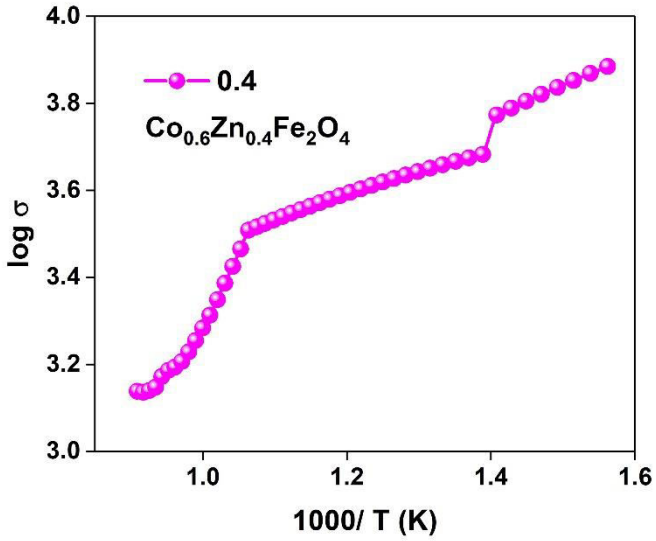

Figure 5 DC-resistivity of $Co_{1-x}Zn_xFe_2O_4$ (x=0.4) nanoparticles

Magnetic property

The M-H plot for $Co_{0.6}Zn_{0.4}Fe_2O_4$ nanoparticles with a composition of (x = 0.4) provides important insights into the magnetic properties of the material. The plot shows a typical S-shaped hysteresis loop, characteristic of ferromagnetic materials, indicating strong magnetic interactions. In **Figure 6**, the saturation magnetization (Ms) is approximately 0.6 emu, representing the maximum magnetization achieved when all magnetic moments are aligned with the applied magnetic field. The coercivity (Hc), or the field strength needed to reduce the magnetization to zero after saturation, is indicated by the points where the curve crosses the x-axis [6]. The remanent magnetization (Mr), which is the residual magnetization when the applied field is reduced to zero, is around 0.3 emu. The significant coercivity and remanence confirm the ferromagnetic behavior of $Co_{0.6}Zn_{0.4}Fe_2O_4$ at room temperature. The shape and size of the hysteresis loop indicate strong magnetic interactions typical of spinel ferrites. The substitution of Zn has a noticeable influence on the magnetic properties, as it affects the distribution of cations between the tetrahedral and octahedral sites in the spinel structure. This change in cation distribution impacts the overall magnetic behavior, confirming that $Co_{0.6}Zn_{0.4}Fe_2O_4$ is a ferromagnetic material with unique magnetic properties due to the incorporation of Zn [21, 22].

International Journal of Innovative Research of Science, Engineering and Technology (IJIRSET)

Impact Factor 8.524

|www.ijirset.com |A Monthly, Peer Reviewed & Referred Journal| e-ISSN: 2319-8753| p-ISSN: 2347-6710|

Volume 13, Issue 9, September 2024

|DOI: 10.15680/IJIRSET.2024.1309044|

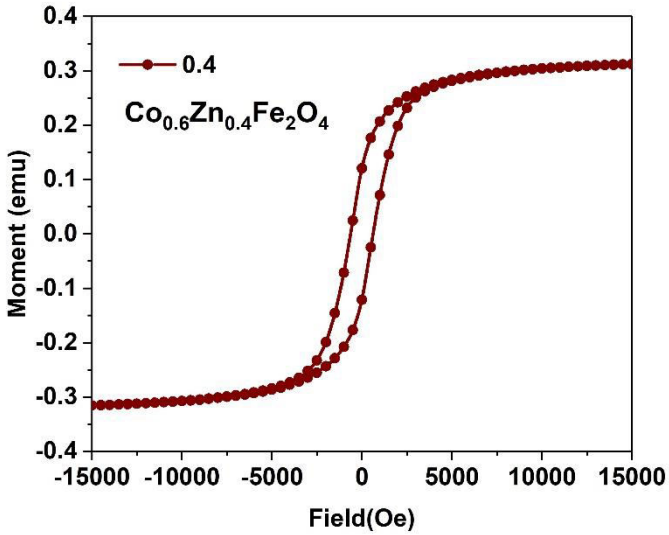

Figure 6 Hysteresis loop of $Co_{1-x}Zn_xFe_2O_4$ (x=0.4) nanoparticles

V. CONCLUSION

In conclusion, the structural and morphological study of $Co_{1-x}Zn_xFe_2O_4$ (x = 0.4) nanoparticles synthesized via a wet chemical method has provided valuable insights into the material's properties. X-ray diffraction confirmed the formation of a single-phase cubic spinel structure, with a stable lattice constant. Fourier-transform infrared spectroscopy (FTIR) indicated characteristic metal-oxygen bond vibrations, affirming the spinel ferrite structure. The crystallite size, dislocation density, and lattice strain, as calculated from XRD data, reveal moderate structural imperfections that may influence the nanoparticles' magnetic properties. Magnetic analysis further demonstrated ferromagnetic behavior, with substantial saturation magnetization, coercivity, and remanent magnetization. The partial substitution of Zn into the $CoFe_2O_4$ lattice led to notable changes in the magnetic characteristics, providing a means to tailor the material's properties for specific applications. Overall, these $Co_{1-x}Zn_xFe_2O_4$ nanoparticles show potential for use in various advanced technologies, including magnetic devices, sensors, and biomedical applications, due to their tunable structural, magnetic, and electrical properties.

REFERENCES

[1] T.T.N. Nha, D.N. Toan, P.H. Nam, D.T. Khan, P.T. Phong, Determine elastic parameters and nanocrystalline size of spinel ferrites MFe2O4 (M= Co, Fe, Mn, Zn) through X-ray diffraction and infrared spectrum: Comparative approach, Journal of Alloys and Compounds, 996 (2024) 174773.
[2] M.A. Darwish, M.M. Hussein, M.K. Omar, W. Abd-Elaziem, Y. Yao, D.S. Klygach, M. Silibin, S.V. Trukhanov, N.V. Abmiotka, D.I. Tishkevich, Crystal structure and peculiarities of microwave parameters of Mg1-xZnxFe2O4 nanospinel ferrites, Ceramics International, 50 (2024) 21027-21039.
[3] R. Arras, K. Sharma, L. Calmels, Interplay between oxygen vacancies and cation ordering in the NiFe 2 O 4 spinel ferrite, Journal of Materials Chemistry C, 12 (2024) 556-561.
[4] M.A.U. Haq, M. Javed, R. Mumtaz, H. Ullah, A. ur Rehman, S.M. Wabaidur, Z. Ahmad, M. Zafar, Mechanical and thermal response of XFe2O4 (X= Zn, Ag and Co) spinel ferrites via IR-spectroscopy and first-principles calculations, Physica Scripta, 99 (2024) 045935.
[5] L. Khudaysh, I.A. Ahmed, S.R. Ejaz, S.A. Khan, Y.A. Haleem, M.M. Ibrahim, M. Ali, H.M.T. Farid, Z.M. El-Bahy, Analysis of cerium substitution in Co–Sr based spinel ferrites for high frequency application, Journal of Rare Earths, 42 (2024) 1755-1763.

International Journal of Innovative Research of Science, Engineering and Technology (IJIRSET)

Impact Factor 8.524

|www.ijirset.com |A Monthly, Peer Reviewed & Referred Journal| e-ISSN: 2319-8753| p-ISSN: 2347-6710|

Volume 13, Issue 9, September 2024

|DOI: 10.15680/IJIRSET.2024.1309044|

[6] A. Soufi, H. Hajjaoui, W. Boumya, A. Elmouwahidi, E. Baillón-García, M. Abdennouri, N. Barka, Recent trends in magnetic spinel ferrites and their composites as heterogeneous Fenton-like catalysts: A review, Journal of Environmental Management, 367 (2024) 121971.
[7] R. Diab, L. El-Deen, M. Nasr, A. El-Hamalawy, A. Abouhaswa, Structural, cation distribution, Raman spectroscopy, and magnetic features of Co-doped Cu–Eu nanocrystalline spinel ferrites, Journal of Materials Science: Materials in Electronics, 35 (2024) 290.
[8] M.M. Rahman, N. Hasan, S. Tabassum, M.H.-O. Rashid, M.H. Rashid, M. Arifuzzaman, Bi3+ Doped Nanocrystalline Ni-Co-Zn Spinel Ferrites: Tuning of Physical, Electrical, Dielectric and Magnetic Properties for Advanced Spintronics Applications, Ceramics International, DOI (2024).
[9] M. Arshad, M. Khalid, M. Younas, Z. Uddin, W. Ullah, I. Boukhris, M. Ashiq, F. Aziz, Physical properties of La3+ ion doped NiZn based spinel ferrite nanomaterials for technological applications, Materials Characterization, 215 (2024) 114210.
[10] H. Badiger, S. Matteppanavar, Pratheek, B. Hegde, Structural, cation distribution, magnetic and electrical properties of Co0. 5Zn0. 5− x Nd x Fe2O4 nano-ferrite, Indian Journal of Physics, 98 (2024) 2363-2374.
[11] A.B. Abou Hammad, A.M. El Nahrawy, Spinel Sensors and Biosensors, Handbook of Nanosensors: Materials and Technological Applications, Springer2024, pp. 427-459.
[12] V.H. Ojha, A.H. Oza, R. Agrawal, R.S. Ningthoujam, Classification of Ferrites, Synthesis and Properties of Spinel Ferrite Nanoparticles and Their Applications, Handbook of Materials Science, Volume 2: Magnetic Materials, Springer2024, pp. 103-146.
[13] A. Salvi, M. Ehsan, P. Thakur, M. Shandilya, A. Thakur, Uses of soft nanoferrites for hyperthermia, Soft Nanoferrites for Biomedical and Environmental Applications, CRC Press, pp. 109-119.
[14] P.A. Vinosha, A. Manikandan, R. Ragu, A. Dinesh, K. Thanrasu, Y. Slimani, A. Baykal, B. Xavier, Impact of nickel substitution on structure, magneto-optical, electrical and acoustical properties of cobalt ferrite nanoparticles, Journal of Alloys and Compounds, 857 (2021) 157517.
[15] A. Messaoudi, A. Omri, A. Benali, M. Ghebouli, A. Djemli, M. Fatmi, A. Habila, A.A. Alothman, N. Hamdaoui, R. Ajjel, Prediction study of structural, thermal, and optical characterization of Co0. 6Zn0. 4Fe2O4 cubic spinel synthesized via sol–gel method for energy storage, Journal of the Korean Physical Society, DOI (2024) 1-11.
[16] B. Jeevanantham, Y. Song, H. Choe, M. Shobana, Structural and optical characteristics of cobalt ferrite nanoparticles, Materials Letters: X, 12 (2021) 100105.
[17] B. Dey, M. Bououdina, P. Dhamodharan, S. AsathBahadur, M. Venkateshwarlu, C. Manoharan, Tuning the gas sensing properties of spinel ferrite NiFe2O4 nanoparticles by Cu doping, Journal of Alloys and Compounds, 970 (2024) 172711.
[18] W. Jdey, N. Hamdaoui, S. Hcini, S. Mansouri, L. El Mir, Enhancement of the Optical properties of Mg0. 6 Cu0. 4 FeCrO4 spinel ferrite via heat treatment, Optical Materials, 147 (2024) 114666.
[19] M. Kamran, M. Anis-ur-Rehman, Resistive switching effect in RE-Doped cobalt ferrite nanoparticles, Ceramics International, 48 (2022) 16912-16922.
[20] T. Pydiraju, K.S. Rao, P.A. Rao, M.C. Varma, A.S. Kumar, K. Rao, Co-Cd nanoferrite for high frequency application with phenomenal rise in DC resistivity, Journal of Magnetism and Magnetic Materials, 524 (2021) 167662.
[21] D.D. Andhare, S.R. Patade, J.S. Kounsalye, K. Jadhav, Effect of Zn doping on structural, magnetic and optical properties of cobalt ferrite nanoparticles synthesized via. Co-precipitation method, Physica B: Condensed Matter, 583 (2020) 412051.
[22] S. Divya, P. Sivaprakash, S. Raja, S.E. Muthu, I. Kim, N. Renuka, S. Arumugam, T.H. Oh, Impact of Zn doping on the dielectric and magnetic properties of CoFe2O4 nanoparticles, Ceramics International, 48 (2022) 33208-33218.

INTERNATIONAL STANDARD SERIAL NUMBER INDIA

INNO SPACE SJIF Scientific Journal Impact Factor

doi crossref

निस्केयर NISCAIR

INTERNATIONAL JOURNAL OF INNOVATIVE RESEARCH

IN SCIENCE | ENGINEERING | TECHNOLOGY

9940 572 462 6381 907 438 ijirset@gmail.com

www.ijirset.com

Scan to save the contact details